Journal of the American Heart Association

ORIGINAL RESEARCH

Aneurysm Wall Enhancement in Unruptured Intracranial Aneurysms: A Histopathological Evaluation

Weiying Zhong, MD; Wenjing Su, MD; Tao Li, MD; Xianjun Tan, MD; Chao Chen, MD; Qian Wang, MD; Donghai Wang, MD; Wandong Su, MD; Yunyan Wang, MD

BACKGROUND: Unruptured intracerebral aneurysm wall enhancement (AWE) on vessel wall magnetic resonance imaging scans may be a promising predictor for rupture-prone intracerebral aneurysms. However, the pathophysiology of AWE remains unclear. To this end, the association between AWE and histopathological changes was assessed in this study.

METHODS AND RESULTS: A total of 35 patients with 41 unruptured intracerebral aneurysms who underwent surgical clipping were prospectively enrolled. A total of 27 aneurysms were available for histological evaluation. The macroscopic and microscopic features of unruptured intracerebral aneurysms with and without enhancement were assessed. The microscopic features studied included inflammatory cell invasion and vasa vasorum, which were assessed using immunohistochemical staining with CD68, CD3, CD20, and myeloperoxidase for the former and CD34 for the latter. A total of 21 (51.2%) aneurysms showed AWE (partial AWE, n=7; circumferential AWE, n=14). Atherosclerotic and translucent aneurysms were identified in 17 and 14 aneurysms, respectively. Aneurysm size, irregularity, and atherosclerotic and translucent aneurysms were associated with AWE on univariate analysis ($P<0.05$). Multivariate logistic regression analysis showed that atherosclerosis was the only factor significantly and independently associated with AWE ($P=0.027$). Histological assessment revealed that inflammatory cell infiltration, intraluminal thrombus, and vasa vasorum were significantly associated with AWE ($P<0.05$).

CONCLUSIONS: Though AWE on vessel wall magnetic resonance imaging scans may be associated with the presence of atherosclerotic lesions in unruptured intracerebral aneurysms, inflammatory cell infiltration within atherosclerosis, intraluminal thrombus, and vasa vasorum may be the main pathological features associated with AWE. However, the underlying pathological mechanism for AWE still needs to be further studied.

Key Words: atherosclerosis ■ inflammation ■ intracranial aneurysm ■ magnetic resonance imaging ■ vasa vasorum

Intracerebral aneurysms (IAs) are histologically characterized by acute and chronic inflammation and vascular wall structure degeneration.[1–3] Increasingly more unruptured IAs have been incidentally discovered and treated,[4] but most of them may be stable and may never rupture over the course of an individual's lifetime. Given the risk associated with treatment and follow-up observation, it is necessary to evaluate the rupture risk and distinguish rupture-prone IAs from those that are stable. IAs may undergo morphological changes before rupture[5]—the current predictors identified are mainly based on the patient and aneurysm characteristics, but these have been proven to have limited predictive value.[6] A good predictor for aneurysm rupture should be easily assessed and can reflect pathological changes in the IA. Recently, it has been reported that aneurysm wall enhancement (AWE) on vessel wall magnetic resonance imaging (MRI) scans, indicating wall inflammation, may reflect the cause of subarachnoid hemorrhage in patients with multiple IAs.[7] This imaging finding is also frequently observed in unstable aneurysms with unfavorable morphological changes

Correspondence to: Wandong Su, MD, and Yunyan Wang, MD, 107 West Culture Road, Jinan, Shandong 250000, China. E-mail: doctorwandongsu@163.com; chendoubo@163.com.

For Sources of Funding and Disclosures, see page 10.

JAHA is available at: www.ahajournals.org/journal/jaha

CLINICAL PERSPECTIVE

What Is New?

- Aneurysm wall enhancement on vessel wall magnetic resonance imaging scans may be associated with atherosclerotic lesions, inflammatory cell infiltration, intraluminal thrombus, and vasa vasorum in unruptured intracerebral aneurysms.

What Are the Clinical Implications?

- We should consider obtaining vessel wall magnetic resonance imaging scans to better understand the pathological characteristics of unruptured intracerebral aneurysms before treatment.
- However, the underlying pathological mechanism for aneurysm wall enhancement still needs to be further studied.

Nonstandard Abbreviations and Acronyms

AWE	aneurysm wall enhancement
MPO	myeloperoxidase
UIA	unruptured intracerebral aneurysm

on follow-up. As such, it may predict an IA prone to rupture.[8,9] However, most evidence is derived from retrospective clinical studies, so whether or not AWE predicts an unstable IA still warrants further research. Above all, we should know the pathological mechanisms related to AWE. Previous studies, including ours, have found that IAs that are symptomatic, larger, and irregularly shaped were associated with AWE[8,10]; however, these variables were still not directly reflective of the pathological changes in IA. To the best of our knowledge, atherosclerosis, inflammation, and vessel wall degenerative changes are important for aneurysm growth and rupture.[1] Recently, studies have also found that these pathological changes, including neovascularization, were associated with AWE.[11–15] However, these previous studies usually included a small number of cases, with scarce pathological assessment. As such, the pathological mechanism underlying AWE still warrants further studies. A previous study showed that myeloperoxidase (MPO), an oxidizing enzyme mainly derived from leukocytes, might serve as a biomarker of a rupture-prone saccular IA wall.[16] Infiltrates of lymphocytes, including T cells and B cells, have been described in aneurysm walls.[2] Herein, we aimed to evaluate the relationship between the pathological features of unruptured intracerebral aneurysms (UIAs), including inflammatory cell infiltration and AWE on vessel wall MRI scans.

METHODS

Patients

This study was approved by the ethics committee of Qilu Hospital of Shandong University. Informed consent was obtained from patients. The data that support the findings of this study are available from the corresponding author on reasonable request. From June 2017 to February 2020, patients with saccular IAs who underwent a preoperative vessel wall MRI and microsurgical clipping were prospectively recruited. All aneurysms had been confirmed by computed tomography angiography or digital subtraction angiography. The exclusion criteria included (1) other types of IAs, like ruptured, dissecting, or fusiform; (2) recurrent aneurysms after coiling or clipping; (3) concomitant vascular diseases, such as vascular malformation, Moyamoya disease, and vasculitis; (4) recent history of aspirin or nonsteroidal anti-inflammatory drug intake; (5) patients with poor quality or incomplete MRI scans for analysis; and (6) aneurysms with poor intraoperative images that were only partially dissected (exposed <50% of their entire dome). Finally, 35 patients with 41 saccular IAs in the anterior circulation were included in this study (among them, some clinical data of 20 cases with 26 UIAs have already been included in our previous study[10]). The patients' demographic characteristics, comorbidities including diabetes mellitus, hypertension, and hyperlipidemia, and radiographic and intraoperative data were collected. The patients' morning fasting venous blood was obtained within 24 hours of admission and lipid profile tests were carried out in our laboratory. The levels of triglycerides, cholesterol, low-density lipoprotein, and high-density lipoprotein were checked. Hypertension was defined in patients taking antihypertensive agents, with a systolic blood pressure of ≥140 mm Hg or diastolic blood pressure of ≥90 mm Hg. Diabetes mellitus was defined in patients taking antidiabetic agents, receiving treatment with insulin injections, with a fasting plasma glucose level of ≥126 mg/dL, a random plasma glucose level of >200 mg/dL, or a hemoglobin A_{1c} level of ≥6.5%. Hyperlipidemia was defined in patients taking lipid lowering drugs, or a fasting plasma cholesterol level of ≥6 mmol/L, a fasting plasma triglyceride level of ≥2 mmol/L, or a fasting plasma low-density lipoprotein level of ≥3.5 mmol/L. Aneurysm size was defined as the maximum measurement from the neck to the dome on computed tomography angiography or digital subtraction angiography. The size, location, and shape irregularity (defined as a saccular aneurysm with a lobular or daughter sac) were assessed before treatment.

Intraoperative Data

Because the complete aneurysmal sac could not easily be harvested during clipping, the atherosclerotic change of UIA was evaluated only by intraoperative inspection in this study. A total of 41 aneurysms underwent microsurgical clipping and the aneurysms were thoroughly explored to observe its gross pathology. The wall features were assessed based on a translucent color and the presence of atherosclerosis in comparison with the appearance of the surrounding healthy parent artery (Figure 1). The aneurysms were divided into atherosclerotic IAs or nonatherosclerotic IA, or translucent or nontranslucent aneurysms. Atherosclerotic IAs were aneurysms with white or yellow areas on the aneurysm wall, and translucent aneurysms were aneurysms with a reddish appearance. If atherosclerotic or translucent lesions involved the whole aneurysm wall, this was considered reflective of a uniform IA. Two experienced neurosurgeons reviewed the intraoperative images independently; any discordance in their interpretations was resolved by discussion.

Histological Data

A total of 27 aneurysmal samples were obtained after microsurgical clipping of the aneurysm neck in this study. The samples were directly fixed in formol, embedded in paraffin and conserved at 4°C. The sample sections (4 μm) were histologically stained with hematoxylin and eosin and Masson. The wall thickness was measured in 27 aneurysms using hematoxylin and eosin. The aneurysms always showed a heterogeneous wall thickness, so the wall thickness was measured at the thickest section of the aneurysm wall in this study. Immunohistochemistry was available in 26 of 27 samples to assess inflammatory reactions and 23 of 27 samples to evaluate vasa vasorum. The deparaffinized sections were incubated with antibodies recognizing CD68+ (a marker of macrophages), MPO (myeloperoxidase, a marker of leukocytes), CD3+ (a marker of T lymphocytes), CD20+ (a marker of B lymphocytes), and CD34+ (a marker of endothelial cells) at 4°C overnight. The sections were then washed 3 times and incubated with secondary antibodies at room temperature for 2 hours. The CD68+, CD3+, CD20+, CD34+, and MPO+ inflammatory cells were then counted from the area that represented the most intensely stained area at a ×10 magnification under a microscope. In this study, a positive cell count ≥5 was considered positive for CD68 and MPO cells and a positive cell count ≥1 was considered positive for CD3, CD20, and CD34 cells. Vasa vasorum was confirmed using hematoxylin and eosin and CD34 stains. The semiquantification was performed by a pathologist blinded to the study.

Magnetic Resonance Imaging

All patients underwent a 3.0-T vessel wall MRI scan (Siemens, Munich, Germany) before microsurgical clipping. First, three-dimensional time-of-flight magnetic resonance angiography was performed to position the aneurysm. Pre- and postcontrast T1-weighted dark-blood fast spin-echo sequence MRI scans were acquired. The scanning parameters used had been presented in our previous study.[10] In this study, AWE was defined as an aneurysm wall signal intensity equal to or greater than that of the pituitary stalk on a postcontrast T1-weighted MRI scan that was not present on the MRI before gadolinium administration (Figure 1). AWE patterns were divided into circumferential (the whole wall was homogeneously enhanced) and partial (part of the wall was enhanced, and the rest was slightly enhanced or not enhanced) enhancement. Two experienced neuroradiologists reviewed the MRI scans independently and determined whether AWE was present or not; any discordance in their interpretations was resolved by discussion.

Statistical Analysis

Data were presented as the median (interquartile range) for continuous variables and frequency for categorical variables. Shapiro-Wilk test was used to assess the normality of continuous variables. If a $P<0.05$, the variable was considered as having a normal distribution. Fisher's exact test for categorical variables and *t* test or Mann-Whitney *U* test for continuous variables were used in this study. First, the clinical, morphologic, and intraoperative characteristics responsible for AWE were evaluated in 35 cases with 41 aneurysms. Factors with $P<0.1$ on univariate analysis were considered as potential independent variables and subsequently included in multivariate logistic regression analysis. Second, the micropathological characteristics responsible for AWE were evaluated in 27 samples using univariate analysis. SPSS version 23 (IBM) was used for statistical analyses. The odds ratio and 95% CIs were calculated. A $P<0.05$ was considered reflective of statistical significance.

RESULTS

Patients

A total of 35 consecutive patients with 41 UIAs were analyzed in this study. The sample consisted of 8 (23%) men and 27 (77%) women, with a median age of 57 years (ranging from 32–72 years). There were 20 (49%) aneurysms in the internal carotid artery, 17 (42%) in the middle cerebral artery, and 4 (10%)

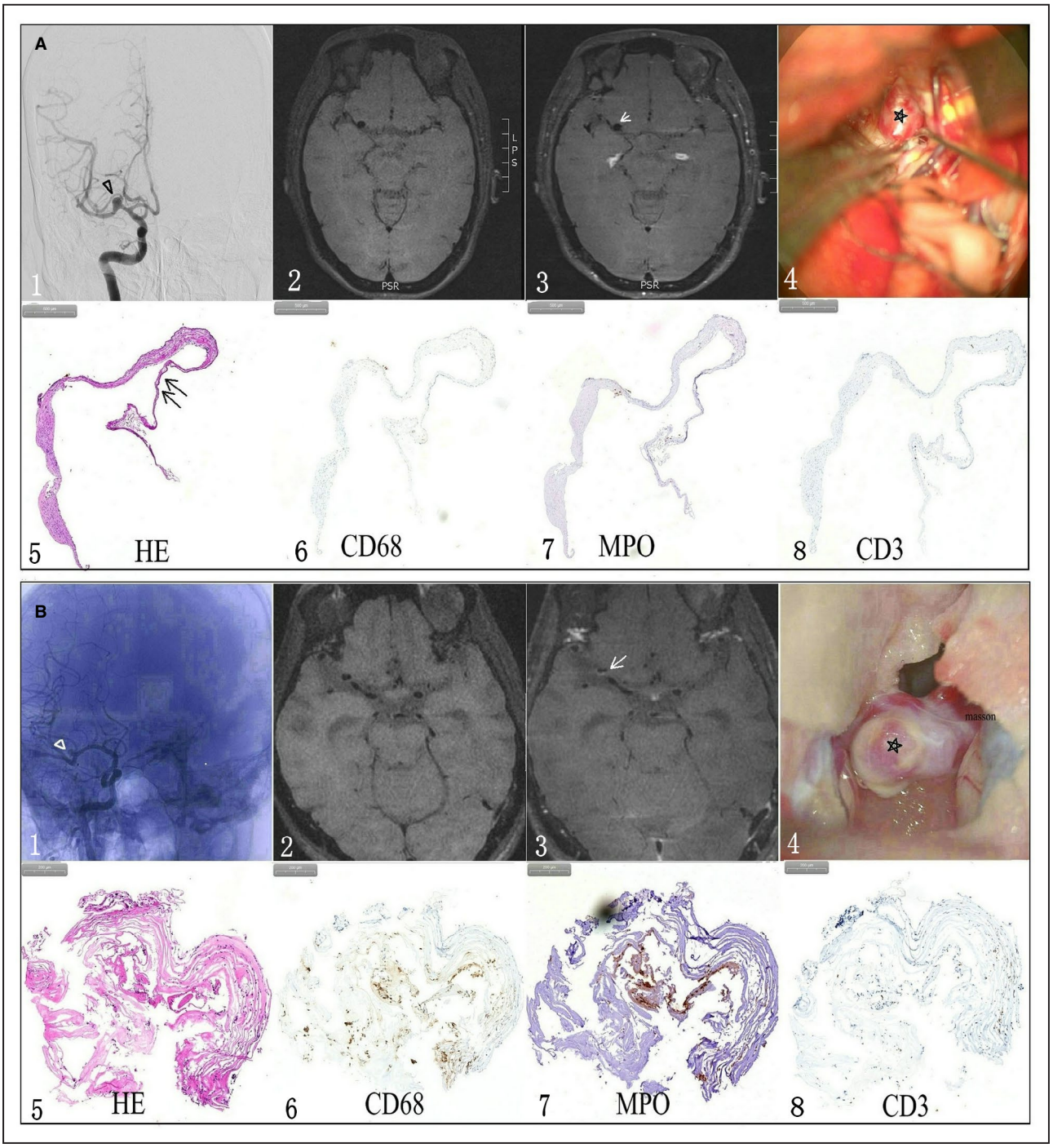

Figure 1. Typical cases illustrating the relationship between pathological features of an unruptured aneurysm and aneurysm wall enhancement (AWE) on vessel wall magnetic resonance imaging (MRI).
A, A woman had a middle artery aneurysm (triangle) (A1) with a reddish appearance wall (star) on intraoperative imaging (A4). Precontrast (A2) and postcontrast (A3) vessel wall MRI showed that the aneurysm wall had nonenhancement (arrow). A hematoxylin and eosin stain (HE) found that the aneurysm wall was extremely thin (double arrow) (A5) without CD68+ macrophage (A6), myeloperoxidase+ (MPO)+ leukocyte (A7) or CD3+ T lymphocyte (A8) infiltration within the aneurysm wall. **B**, a man had a middle artery aneurysm (triangle) (B1) with an atherosclerotic appearance wall (star) on intraoperative imaging (B4). Precontrast (B2) and postcontrast (B3) MRI scans showed the aneurysm had partial enhancement (arrow) on postcontrast vessel wall MRI. Histological study (HE) found that the aneurysm wall was heterogeneous and deranged (B5). Inflammatory cells, including CD68+ macrophages (B6), MPO+ leukocytes (B7) and CD3+ T lymphocytes (B8), were noticed within aneurysm wall.

in the anterior cerebral artery. The median size was 6.20 mm (ranging from 2.5–23.3 mm). Irregular morphology was detected in 16 (39%) aneurysms. A total of 20 aneurysms (49%) showed nonenhancement on vessel wall MRI scans and 21 (51%) showed AWE. In cases with AWE, 7 (33%) aneurysms showed partial AWE and 14 (67%) showed circumferential AWE. There is no difference in clinical comorbidity or the level of blood lipids between aneurysms with or without enhancement (Table 1). The size and morphology of aneurysms were significantly associated with AWE in this study. The median size of aneurysms with AWE was 9.2 mm (ranging from 4.0–23.3 mm), whereas it was 4.35 (ranging from 2.5–11.2 mm) in aneurysms without AWE (P<0.001). The proportion of irregular shapes in AWE aneurysms was higher than that in aneurysms without AWE (62% [13/21] versus 15% [3/20], respectively; P=0.004).

Intraoperative Characteristics of UIAs With and Without Enhancement

Atherosclerotic aneurysms were identified in 17/41 (42%) aneurysms, including 14 aneurysms with yellow changes and 3 with white changes, which was significantly associated with aneurysm size (P=0.006) but not with any comorbidity or level of blood lipids (P>0.05). As Table 1 shows, atherosclerotic aneurysms are significantly associated with AWE; 15 out of 17 (88%) atherosclerotic aneurysms had AWE (P=0.000093), and all 9 uniform atherosclerotic aneurysms had AWE. The proportion of atherosclerotic aneurysms was 71.43% (15/21) and 10% (2/20) in aneurysms with and without AWE, respectively (P=0.001).Translucent aneurysms were noticed in 14/41 (34%) aneurysms, which was negatively associated with aneurysm size and AWE (P<0.05). Only 2 translucent aneurysms (14%) had AWE in our study. Variables such as the aneurysm size, irregular shape, and atherosclerotic and translucent aneurysms were then included in multivariate logistic regression analysis. This analysis showed that atherosclerotic lesions within aneurysms (odds ratio, 34.1; 95% CI, 1.5–769.3) are the only factor significantly and independently associated with AWE (P=0.027) (Table 2). Receiver operating characteristic curve of univariate and multivariate analyses indicated that aneurysm size, irregular shape, and atherosclerotic and translucent aneurysms probably predicted AWE on vessel wall MRI (P<0.05) (Figure 2). A multivariate model (including the preceding 4 univariates) probably further improved the prediction of AWE in this study (area under the curve, 0.971; 95% CI, 0.919–1.000; P<0.001).The morphologic and intraoperative characteristics responsible for AWE patterns were also studied in aneurysms with AWE.

Table 1. The Clinical, Morphologic, and Intraoperative Characteristics of Unruptured Intracranial Aneurysms With and Without Aneurysm Wall Enhancement

Characteristics	Aneurysm Groups (N=41)		*P* Value
	Nonenhancement (n=20)	Enhancement (n=21)	
Age, y	54±9	58±8	0.132
Female, n (%)	18 (90)	14 (67)	0.130
Current smoking (%)	2 (10)	5 (24)	0.410
Diabetes mellitus (%)	3 (15)	2 (10)	0.663
Hypertension (%)	10 (50)	8 (38)	0.536
Hyperlipidemia (%)	3 (15)	7 (33)	0.277
Cholesterol, mmol/L	4.12 (3.53–4.71)	4.49 (3.74–6.28)	0.246
Triglycerides, mmol/L	1.40 (1.14–1.73)	1.50 (0.98–2.78)	0.514
Low-density lipoprotein, mmol/L	2.56 (1.83–2.81)	2.82 (2.01–3.75)	0.155
High-density lipoprotein, mmol/L	1.19 (0.98–1.40)	1.14 (1.05–1.33)	0.584
Location			
Internal carotid artery (%)	8 (40)	12 (57)	
Middle cerebral artery (%)	10 (50)	7 (33)	0.521
Anterior cerebral artery (%)	2 (10)	2 (10)	
Size, mm*	4.4 (3.5–5.6)	9.2 (7.6–11.9)	< 0.001
Irregular aneurysms* (%)	3 (15)	13 (62)	0.004
Atherosclerotic intracerebral aneurysms* (%)	2 (10)	15 (71)	< 0.001
translucent aneurysms* (%)	12 (60)	2 (10)	0.001

Variables are expressed as the median (interquartile range) or number of aneurysms (%).
*Statistically significant.

Table 2. Multivariate Logistic Regression Analysis of Variables Independently Associated With Aneurysm Wall Enhancement

Variable	Odds Ratio	95% CI	*P* Value
Size	1.6	0.916–2.933	0.096
Irregular aneurysm	14.3	0.629–325.461	0.095
Atherosclerotic aneurysm	34.1	1.509–769.316	0.027*
Translucent aneurysms	0.01	0.003–1.077	0.056

*Statistically significant.

We found that the 3 variables mentioned previously (size, irregularity, atherosclerotic versus translucent aneurysm) are not associated with partial or circumferential enhancement (P>0.05) (Table 3). The proportion of atherosclerotic aneurysms revealed no significant difference in aneurysms with partial and circumferential AWE (86% [12/14] versus 43% [3/7], respectively; P=0.12). Even uniform atherosclerotic aneurysms did not appear to have circumferential AWE in this study. The proportion of uniform atherosclerotic aneurysms in aneurysms with partial AWE was not significantly different than that in aneurysms with circumferential AWE (29% [2/7] versus 50% [7/14], respectively; P=0.642).

Histological Characteristics of UIAs With and Without Enhancement

A total of 27 aneurysm specimens were harvested to study the histological characteristics for AWE. The median wall thickness was 149.97 μm (ranging from 18.43 to 420.91 μm), which was significantly associated with atherosclerosis (P=0.003) but not significantly associated with AWE in this study (P=0.124) (Table 4). The mean wall thickness was not significantly different in aneurysms with AWE and aneurysms without AWE (193.17±120.48 μm versus 122.29±94.08 μm, respectively). An intraluminal thrombus was noticed in 10/27 (37%) aneurysms using hematoxylin and eosin and Masson stains, which was significantly associated with aneurysm size (P=0.017) and AWE (P=0.012) (Figure 3). The proportion of cases with signs of intraluminal thrombus was 53% (10/19) and 0% (0/8) in aneurysms with and without AWE, respectively. Immunohistochemical staining was available in 26 of 27 specimens, except for CD34 staining, wherein only 23 were available. A cluster distribution of inflammatory cells was noticed in some aneurysm walls (Figure 4). CD68+ was identified in 20/26 (77%) aneurysms, MPO+ in 21/26 (81%) aneurysms, CD3+ in 12/26 (46%) aneurysms, and CD20+ in 8/26 (31%) lesions. CD68 and MPO positivity was significantly associated with AWE (P<0.05) (Table 4).

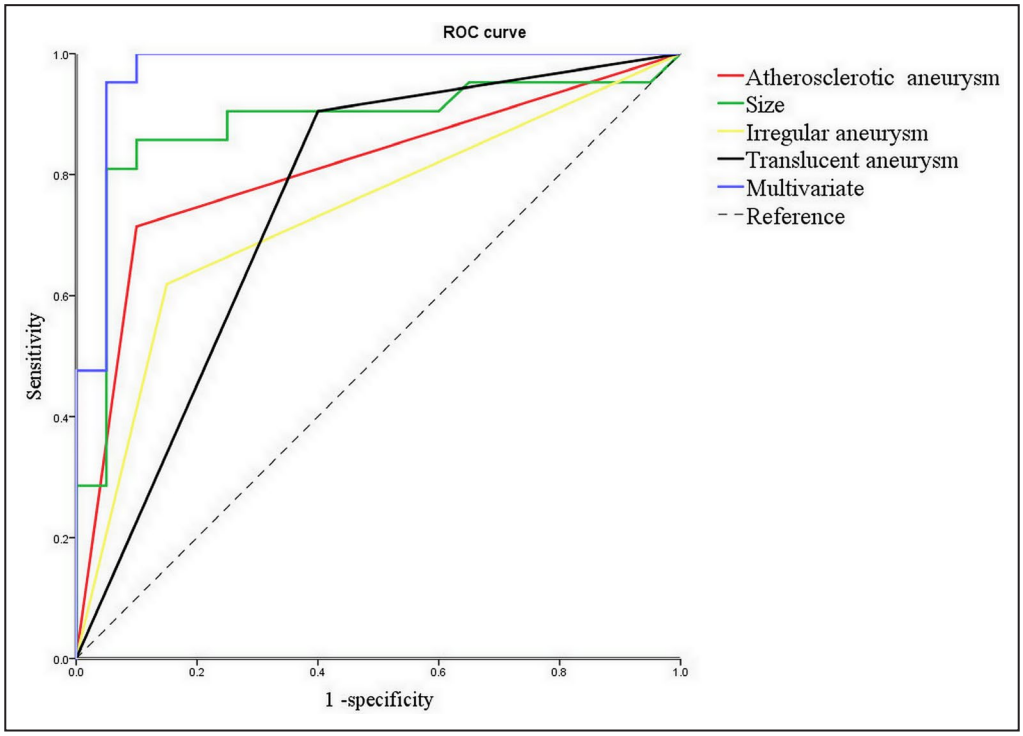

Figure 2. The prediction curve of the independent variables for aneurysm wall enhancement (AWE).
Receiver operating characteristic (ROC) curve of univariate and multivariate for AWE on vessel wall magnetic resonance imaging (MRI) indicated that atherosclerotic aneurysms probably predicted AWE on vessel wall MRI (P<0.05).

Table 3. The Intraoperative Characteristics of Unruptured Intracranial Aneurysms With Partial Enhancement and With Circumferential Enhancement

Characteristics	Aneurysm Groups (N=21)		*P* Value
	Partial Enhancement (n=7)	Circumferential Enhancement (n=14)	
Size, mm	8.5 (7.4–9.2)	10.7 (7.5–13.7)	0.192
Irregular aneurysm	6 (86)	7 (50)	0.174
Atherosclerotic aneurysm	3 (43)	12 (86)	0.120
Translucent aneurysm	1 (14)	1 (7)	>0.999

Variables are expressed as the median (interquartile range) or number of aneurysms (%).

Further analysis showed that both CD68 and MPO positivity was also significantly associated with AWE in this study. The proportion of both CD68 and MPO positivity in aneurysms with and without AWE was 89% (17/19) and 29%(2/7), respectively; *P*=0.006. However, T and B lymphocyte positivity was not associated with AWE (*P*>0.05). Vasa vasorum was identified in 14/23 (61%) aneurysms, mainly in the adventitia of the aneurysm wall or in the intraluminal thrombus; it was also significantly associated with AWE (*P*=0.018). Further analysis showed that CD68 positivity was significantly associated with atherosclerotic aneurysms (*P*=0.018). A similar trend was also identified for MPO positivity (*P*=0.055). T and B lymphocyte positivity was found to not be associated with atherosclerotic aneurysms (*P*>0.05).

DISCUSSION

We found that aneurysms with atherosclerotic lesions were significantly and independently associated with AWE in this study. The histological features including acute and chronic inflammatory cell infiltration, vasa vasorum, and intraluminal thrombus were also associated with AWE.

Table 4. Histological Characteristics of Unruptured Intracranial Aneurysms With and Without Aneurysm Wall Enhancement

	Nonenhancement	Enhancement	*P* Value
Wall thickness, μm	91.88 (53.82–152.82)	187.16 (85.07–277.83)	0.124
Intraluminal thrombus	0/8 (0)	10/19 (53)	0.012*
CD68	2/7 (29)	18/19 (95)	0.002*
Myeloperoxidase	3/7 (43)	18/19 (95)	0.001*
CD3	1/7 (14)	11/19 (57)	0.081
CD20	1/7 (14)	7/19 (37)	0.375
CD34	1/6 (17)	13/17 (76)	0.018*

Variables are expressed as the median (interquartile range) or number of aneurysm (%).

*Statistically significant.

Atherosclerosis changes were frequently identified in IAs, and aneurysms with atherosclerosis usually presented with thick aneurysm walls in our study. Previous studies, including ours, also found that the presence of atherosclerotic lesions was associated with AWE.[11,13] However, the presence of atherosclerotic lesions within aneurysms was not associated with AWE patterns. Uniform atherosclerotic aneurysm did not always lead to circumferential enhancement in this study, so atherosclerosis may not be the direct pathological mechanism underlying AWE. To the best of our knowledge, inflammation is involved in the process of atherosclerosis and aneurysm formation.[2] Inflammatory infiltration was associated with atherosclerotic aneurysms in this study, and a previous study on histopathology, including ours, also found that inflammatory infiltrates in the form of macrophages and leukocytes within IA walls were strongly associated with AWE.[13,17] As such, inflammation within atherosclerotic aneurysm walls may be responsible for AWE in such aneurysms. Inflammation has been considered a potential cause for wall degeneration that predisposes to rupture,[3] and intracerebral AWE on vessel wall MRI scans may be a promising predictor of a rupture-prone IA. Because of complex and changing hemodynamics, especially within larger aneurysms, there may be temporal and spatial differences in wall inflammation. In addition, atherosclerotic changes and wall thickness are variable, so not all atherosclerotic aneurysms have AWE in our study. This is why uniform atherosclerotic aneurysms are not always associated with circumferential enhancement, and a thickened aneurysm wall was not associated with AWE in this study.

In our study, translucent aneurysms were less likely to have AWE. A linear correlation between aneurysm wall signal intensity and histological thickness had been previously reported.[18] A thickened vessel wall is more easily detected, whereas MRI resolution may be insufficient to evaluate very thin aneurysm walls. The degree of enhancement would be weakened because of a partial volume effect. However, we found that translucent aneurysms were significantly smaller than their nontranslucent counterparts; similar results were

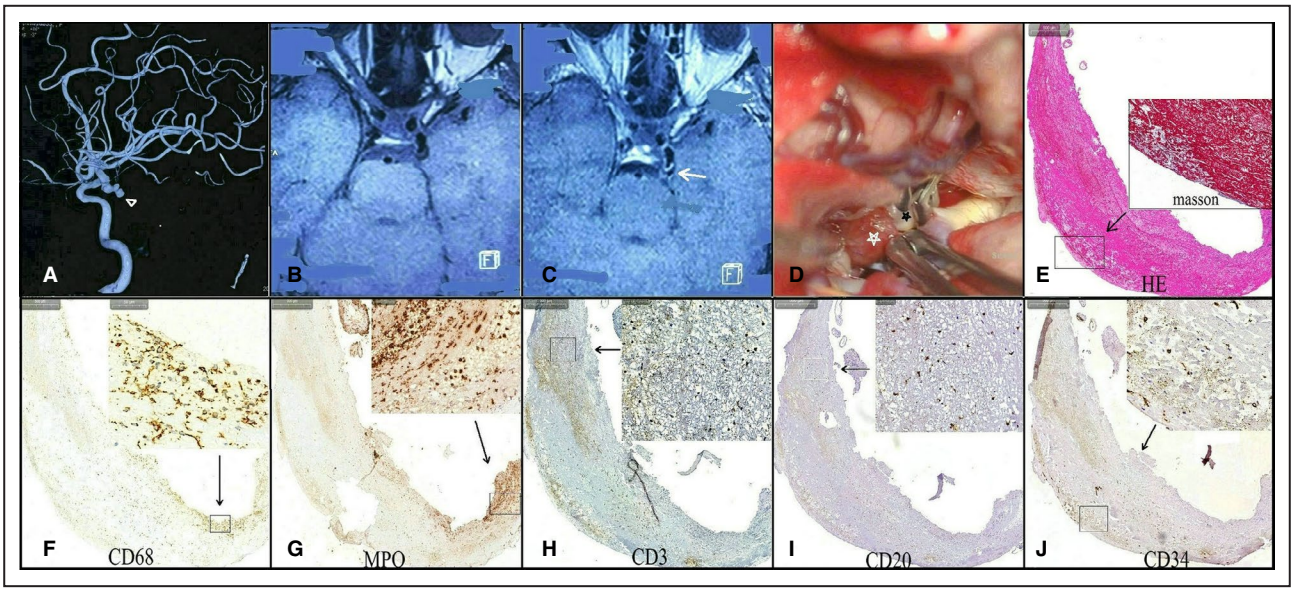

Figure 3. A woman had a posterior communicating aneurysm with oculomotor nerve palsy (triangle arrow).
(**A**) Precontrast (**B**) and postcontrast (**C**) magnetic resonance imaging scans showed that the aneurysm was strongly enhanced (arrow). Intraoperative imaging (**D**) showed that the aneurysm wall had an atherosclerotic change (black star) with a daughter sac thrombosis (white star). Hematoxylin and eosin stain and Masson stains (**E**) found that the daughter sac contained extremely thin fibrous tissue with a massive intraluminal thrombus. Different types of inflammatory cells, including CD68+ macrophages (**F**), myeloperoxidase+ (MPO+) leukocytes (**G**), CD3+ T lymphocytes (**H**), and CD20+ B lymphocytes (**I**), were noticed within the thrombosis. A CD34 stain (**J**) indicated neovascularization within thrombosis.

also found in a previous study.[19] Inflammation may be not the main pathological mechanism underlying small translucent aneurysm remodeling. A small aneurysm is usually associated with fast blood flow and high wall shear stress, and the latter can trigger mural cell-mediated but not inflammation-mediated degenerative remodeling in these aneurysms.[20] Therefore, walls of translucent aneurysms were less likely to be enhanced on vessel wall MRI scans. Therefore, there is some limitation to evaluating small and thin aneurysm walls using vessel wall imaging, as aneurysms without AWE are not always stable and not all ruptured IAs showed absence AWE.[21] The interpretation of unruptured IAs without wall enhancement still warrants further study.

As our study has revealed, vasa vasorum was frequently noticed in aneurysms, especially in the large ones. Normally, the intracranial vasa vasorum does not exist at birth but develops in adulthood when the vessels thicken and become diseased.[22] Vasa vasorum not only transports contrast agents but also inflammatory cells into diseased aneurysm walls. Meanwhile, the vasa vasorum is usually immature and fragile, is prone to rupture, and induces microhemorrhages and extravasation of blood constituents,[23] after which the induced inflammation further increases the leakage and accumulation of contrast agents within the aneurysm wall, affecting wall enhancement.

Thrombus formation is also frequently histologically demonstrated within the luminal surface of the IA wall, especially in larger aneurysms. The aneurysm usually lacks an intact endothelium, and the loss of an intact endothelial layer may expose thrombogenic matrix surfaces and predispose to thrombus formation.[24] The presence of thrombosis has been suggested as a biomarker for aneurysm instability and rupture.[25] The entrapped blood constituents within a thrombus, such as neutrophils, may not only release cytokines and proteases leading to cell death and chronic proteolysis of the aneurysm wall but may also release peroxidases, leading to enhanced inflammation and oxidative stress within the aneurysm wall.[1,16] In addition, because of the enhanced inflammation and stagnant blood flow in larger aneurysms, the contrast agents are more likely to penetrate the unorganized thrombus and the underlying aneurysm wall. An intraluminal thrombus is also important for the formation of vasa vasorum. A double-rim enhancement on high-resolution enhanced 7T MRI has been suggested to represent a thrombus aneurysm in the literature.[25] However, this may be depend on the stage and volume of thrombus and spatial resolution of the MRI scan, and the turbulent slow blood flow within larger aneurysms might also induce contrast stagnation along the vessel wall; a combination enhancement due to slow flow and inflammation should be not excluded.[26]

Even if there are obvious atherosclerotic changes and inflammatory cell infiltrates in an aneurysm wall, because of an aneurysm's complex morphological and hemodynamic characteristics, the said wall may not always be enhanced under the defined MRI parameters,

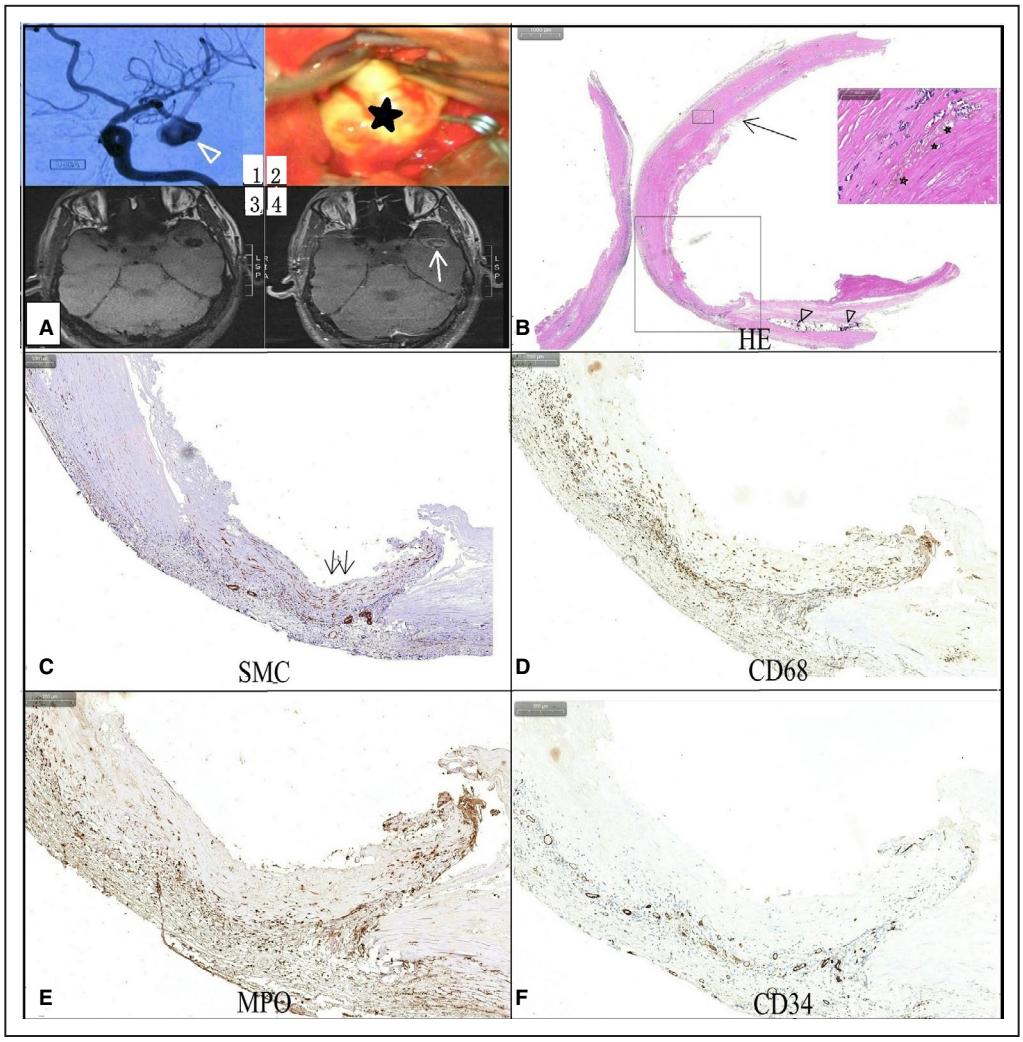

Figure 4. A man had a middle artery aneurysm (triangle arrow).
(**A1**) with a uniform atherosclerosis appearance (star) on intraoperative imaging (**A2**), which had significant enhancement (arrow) on postcontrast vessel wall magnetic resonance imaging (**A4**). A hematoxylin and eosin stain (**B**) showed the thickened aneurysm wall contained hemosiderosis (star) and calcification (triangle). A vascular smooth muscle cells (SMC) stain (**C**) indicated hyperplasia and derangement of SMCs within the aneurysm wall (double arrow). Clustered inflammatory cells, including CD68+ macrophages (**D**), myeloperoxidase+ (MPO+) leukocytes (**E**), and T and B lymphocytes, were noticed within the aneurysm wall, and CD34 stain (**F**) indicated plenty of neovascularization within the aneurysm wall.

meaning that personalized parameters, such as delay alternating with nutation for tailored excitation or scan time after gadolinium is administered,[27] should be considered in some complex aneurysms. Meanwhile, the surrounding structures, such as the dura and adjacent veins may be confused with wall enhancement.[26] There are limitations to evaluating small and thin aneurysms, and a comprehensive assessment for these small aneurysms, including flow dynamics, should be considered.

There are some other limitations to this study. First, the included aneurysm number in our study was small, which would influence our statistical results. As our study showed, the CI for atherosclerotic aneurysm was wide. However, the observed odds ratio was still meaningful as we have adjusted the effects of other variables using multivariate analysis. More samples are needed to determine a more robust estimate in the future. Second, only large aneurysms had histological findings. Few small aneurysms were included in this study, and the included aneurysms involved only the anterior circulation; as such, selection bias may exist. Third, aneurysms could not always be completely exposed before clipping in some cases, which could influence the assessment. Meanwhile, not all the samples were entirely used for histological study, meaning that it is difficult to preserve the morphology of the aneurysm tissue for histological assessment, and the pathological features may not reflect the

entire characteristics of the aneurysm. Finally, the use of statins to reduce hyperlipidemia may also affect inflammation of UIAs, which might influence our results. However, this study still provides some pathological evidence for AWE on vessel wall MRI scans.

CONCLUSIONS

Though AWE on vessel wall MRI scans may be associated with the presence of atherosclerotic lesions in UIAs, inflammatory cell infiltration within atherosclerosis, intraluminal thrombus, and vasa vasorum may be the main pathological features associated with AWE. However, the underlying pathological mechanism for AWE still needs to be further studied.

ARTICLE INFORMATION

Received July 30, 2020; accepted November 3, 2020.

Affiliations

From the Department of Neurosurgery, Qilu Hospital of Shandong University and Institute of Brain and Brain-Inspired Science, Shandong University, Jinan, Shandong Province, China (W.Z., C.C., D.W., W.S., Y.W.); Shandong Key Laboratory of Brain Function Remodeling, Jinan, Shandong Province, China (W.Z., C.C., D.W., W.S., Y.W.); Department of Pathology, Shandong Provincial Hospital affiliated with Shandong University, Jinan, Shandong Province, China (W.S.); Department of Neurosurgery, The No. 4 People's Hospital of Jinan, Jinan, Shandong Province, China (T.L.); Department of Neurosurgery, People's Hospital of Chiping City, Liaocheng, Shandong Province, China (X.T.); and Department of Radiology, Qilu Hospital of Shandong University, Jinan, Shandong Province, China (Q.W.).

Sources of Funding

This study was funded by the National Natural Science Foundation of China (Grant number: 81701160).

Disclosures

None.

REFERENCES

1. Frösen J, Tulamo R, Paetau A, Laaksamo E, Korja M, Laakso A, Niemelä M, Hernesniemi J. Saccular intracranial aneurysm: pathology and mechanisms. *Acta Neuropathol*. 2012;123:773–786.
2. Sawyer DM, Amenta PS, Medel R, Dumont AS. Inflammatory mediators in vascular disease: identifying promising targets for intracranial aneurysm research. *Mediators Inflamm*. 2015;2015:1–10.
3. Chalouhi N, Hoh BL, Hasan D. Review of cerebral aneurysm formation, growth, and rupture. *Stroke*. 2013;44:3613–3622.
4. Luther E, McCarthy DJ, Brunet M-C, Sur S, Chen SH, Sheinberg D, Hasan D, Jabbour P, Yavagal DR, Peterson EC, et al. Treatment and diagnosis of cerebral aneurysms in the post-International Subarachnoid Aneurysm Trial (ISAT) era: trends and outcomes. *J Neurointerv Surg*. 2020;12:682–687.
5. Frösen J, Piippo A, Paetau A, Kangasniemi M, Niemelä M, Hernesniemi J, Jääskeläinen J. Remodeling of saccular cerebral artery aneurysm wall is associated with rupture: histological analysis of 24 unruptured and 42 ruptured cases. *Stroke*. 2004;35:2287–2293.
6. Bijlenga P, Gondar R, Schilling S, Morel S, Hirsch S, Cuony J, Corniola MV, Perren F, Rüfenacht D, Schaller K. PHASES score for the management of intracranial aneurysm: a cross-sectional population-based retrospective study. *Stroke*. 2017;48:2105–2112.
7. Matouk CC, Mandell DM, Günel M, Bulsara KR, Malhotra A, Hebert R, Johnson MH, Mikulis DJ, Minja FJ. Vessel wall magnetic resonance imaging identifies the site of rupture in patients with multiple intracranial aneurysms: proof of principle. *Neurosurgery*. 2013;72:492–496.
8. Vergouwen MDI, Backes D, van der Schaaf IC, Hendrikse J, Kleinloog R, Algra A, Rinkel GJE. Gadolinium enhancement of the aneurysm wall in unruptured intracranial aneurysms is associated with an increased risk of aneurysm instability: a follow-up study. *AJNR Am J Neuroradiol*. 2019;40:1112–1116.
9. Matsushige T, Shimonaga K, Ishii D, Sakamoto S, Hosogai M, Hashimoto Y, Kaneko M, Ono C, Mizoue T, Kurisu K. Vessel wall imaging of evolving unruptured intracranial aneurysms. *Stroke*. 2019;50:1891–1894.
10. Zhong W, Du Y, Guo Q, Tan X, Li T, Chen C, Liu M, Shen J, Su W, Wang D, et al. The clinical and morphologic features related to aneurysm wall enhancement and enhancement pattern in patients with anterior circulation aneurysms. *World Neurosurg*. 2020;134:e649–e656.
11. Hashimoto Y, Matsushige T, Shimonaga K, Hosogai M, Kaneko M, Ono C, Mizoue T. Vessel wall imaging predicts the presence of atherosclerotic lesions in unruptured intracranial aneurysms. *World Neurosurg*. 2019;132:e775–e782.
12. Shimonaga K, Matsushige T, Ishii D, Sakamoto S, Hosogai M, Kawasumi T, Kaneko M, Ono C, Kurisu K. Clinicopathological insights from vessel wall imaging of unruptured intracranial aneurysms. *Stroke*. 2018;49:2516–2519.
13. Quan K, Song J, Yang Z, Wang D, An Q, Huang L, Liu P, Li P, Tian Y, Zhou L, et al. Validation of wall enhancement as a new imaging biomarker of unruptured cerebral aneurysm. *Stroke*. 2019;50:1570–1573.
14. Larsen N, von der Brelie C, Trick D, Riedel CH, Lindner T, Madjidyar J, Jansen O, Synowitz M, Flüh C. Vessel wall enhancement in unruptured intracranial aneurysms: an indicator for higher risk of rupture? high-resolution MR imaging and correlated histologic findings. *AJNR Am J Neuroradiol*. 2018;39:1617–1621.
15. Hu P, Yang Q, Wang DD, Guan SC, Zhang HQ. Wall enhancement on high-resolution magnetic resonance imaging may predict an unsteady state of an intracranial saccular aneurysm. *Neuroradiology*. 2016;58:979–985.
16. Ollikainen E, Tulamo R, Lehti S, Hernesniemi J, Niemelä M, Kovanen PT, Frösen J. Myeloperoxidase associates with degenerative remodeling and rupture of the saccular intracranial aneurysm wall. *J Neuropathol Exp Neurol*. 2018;77:461–468.
17. Hudson JS, Zanaty M, Nakagawa D, Kung DK, Jabbour P, Samaniego EA, Hasan D. Magnetic resonance vessel wall imaging in human intracranial aneurysms. *Stroke*. 2019;50:e1.
18. Kleinloog R, Korkmaz E, Zwanenburg JJM, Kuijf HJ, Visser F, Blankena R, Post JA, Ruigrok YM, Luijten PR, Regli L, et al. Visualization of the aneurysm wall: a 7.0-tesla magnetic resonance imaging study. *Neurosurgery*. 2014;75:614–622.
19. Song J, Park JE, Kim HR, Shin YS. Observation of cerebral aneurysm wall thickness using intraoperative microscopy: clinical and morphological analysis of translucent aneurysm. *Neurol Sci*. 2015;36:907–912.
20. Meng H, Tutino VM, Xiang J, Siddiqui A. High WSS or low WSS? complex interactions of hemodynamics with intracranial aneurysm initiation, growth, and rupture: toward a unifying hypothesis. *AJNR Am J Neuroradiol*. 2014;35:1254–1262.
21. Texakalidis P, Hilditch CA, Lehman V, Lanzino G, Pereira VM, Brinjikji W. Vessel wall imaging of intracranial aneurysms: systematic review and meta-analysis. *World Neurosurg*. 2018;117:453–458.
22. Yang WJ, Wong KS, Chen XY. Intracranial atherosclerosis: from microscopy to high-resolution magnetic resonance imaging. *J Stroke*. 2017;19:249–260.
23. Ollikainen E, Tulamo R, Frösen J, Lehti S, Honkanen P, Hernesniemi J, Niemelä M, Kovanen PT. Mast cells, neovascularization, and microhemorrhages are associated with saccular intracranial artery aneurysm wall remodeling. *J Neuropathol Exp Neurol*. 2014;73:855–864.
24. Aksu K, Donmez A, Keser G. Inflammation-induced thrombosis: mechanisms, disease associations and management. *Curr Pharm Des*. 2012;18:1478–1493.
25. Sato T, Matsushige T, Chen B, Gembruch O, Dammann P, Jabbarli R, Forsting M, Junker A, Maderwald S, Quick HH, et al. Wall contrast enhancement of thrombosed intracranial aneurysms at 7T MRI. *AJNR Am J Neuroradiol*. 2019;40:1106–1111.
26. Santarosa C, Cord B, Koo A, Bhogal P, Malhotra A, Payabvash S, Minja FJ, Matouk CC. Vessel wall magnetic resonance imaging in intracranial aneurysms: principles and emerging clinical applications. *Interv Neuroradiol*. 2020;26:135–146.
27. Xie Y, Yang Q, Xie G, Pang J, Fan Z, Li D. Improved blackblood imaging using DANTE-SPACE for simultaneous carotid and intracranial vessel wall evaluation. *Magn Reson Med*. 2020;75:2286–2294.